The Journal of Veterinary Medical Science

FULL PAPER

Avian Pathology

Distribution of lesions in psittacine birds naturally infected with parrot bornavirus in Japan

Chinatsu FUJIWARA[1)#], Naoyuki AIHARA[1)#], Motokazu YOSHINO[1)], Takanori SHIGA[1)], Kan FUJINO[2)], Ryo KOMORIZONO[3)], Akiko MAKINO[3,4)], Keizo TOMONAGA[3–5)], Reiko SOGA[3,6)], Junichi KAMIIE[1)*]

[1)]Laboratory of Veterinary Pathology, School of Veterinary Medicine, Azabu University, Kanagawa, Japan
[2)]Laboratory of Microbiology, Department of Veterinary Medicine, School of Veterinary Medicine, Azabu University, Kanagawa, Japan
[3)]Laboratory of RNA Viruses, Department of Virus Research, Institute for Life and Medical Sciences (LiMe), Kyoto University, Kyoto, Japan
[4)]Laboratory of RNA Viruses, Department of Mammalian Regulatory Network, Graduate School of Biostudies, Kyoto University, Kyoto, Japan
[5)]Department of Molecular Virology, Graduate School of Medicine, Kyoto University, Kyoto, Japan
[6)]Grow-Wing Animal Hospital, Kanagawa, Japan

ABSTRACT. Mononuclear cell infiltration of the central nervous system and ganglioneuritis are characteristic histopathological findings of proventricular dilatation disease (PDD) caused by parrot bornavirus (PaBV) infection. The purpose of this study was to clarify the link between the degree of inflammatory lesions and the distribution of the virus antigen in naturally PaBV-infected parrots. Pathological examination was performed on 18 PaBV-infected birds identified by reverse transcriptase-PCR. Dilatation of the crop, proventriculus, and ventriculus was observed in all 18 (100%) birds, and dilation of the right ventricle of the heart was observed in 14/18 (78%) birds. Cases were classified based on the scores for the distribution and degree of histological lesions into neural type, with severe brain lesions, digestive type, with severe gastric lesions, or nervous/digestive type, with severe lesions in both the brain and ventriculus. The PaBV immunohistological score correlated with the inflammatory lesion scores. Ganglioneuritis, myocarditis, and myocardial degeneration were frequently observed in the heart. Interestingly, macroscopic and microscopic lesions and virus antigen were detected in the hearts of all three histological types. The present study showed that parrots naturally infected with PaBVs can be grouped into three types based on the lesion distribution, and heart failure is an important symptom in PaBV-infected parrots.

KEYWORDS: avian ganglioneuritis, cardiac lesion, lesion distribution, natural infection, parrot bornavirus

J Vet Med Sci
86(11): 1110–1118, 2024
doi: 10.1292/jvms.24-0061

Received: 8 February 2024
Accepted: 8 September 2024
Advanced Epub:
27 September 2024

In 2008, a nucleic acid sequence similar to the Borna disease virus 1 sequence was detected in parrots diagnosed with proventricular dilatation disease (PDD) [4, 6]. This sequence similarity led to the identification of parrot avian bornaviruses, some of which were determined as the causative agents of PDD. Among avian bornaviruses, parrot bornaviruses (PaBVs) classified as the species *Orthobornavirus alphapsittaciforme* and *Orthobornavirus betapsittaciforme* encompass eight distinct viruses, namely PaBV-1 to -8, which are the major viruses causing PDD in parrots [8, 12, 16]. PDD, which affects captive populations of psittacine birds worldwide, is a lethal disease exhibiting neurological disorders, including depression, ataxia, and seizures, and digestive disorders, such as weight loss and regurgitation [5]. The characteristic histopathological findings of PDD, which correlate with the symptoms, include mononuclear cell infiltration of the central nervous system and myenteric ganglioneuritis in the gastrointestinal tract [1, 14]. Ganglioneuritis is also observed in other organs, including the adrenal gland, heart, spleen, liver, kidney, lungs, pancreas, testes, ovary, skeletal muscle, and skin [1].

*Correspondence to: Kamiie J: kamiie@azabu-u.ac.jp, Laboratory of Veterinary Pathology, School of Veterinary Medicine, Azabu University, 1-17-71 Fuchinobe, Chuo-ku, Sagamihara, Kanagawa 252-5201, Japan
#These authors contributed equally to this work.
(Supplementary material: refer to J-STAGE: https://www.jstage.jst.go.jp/browse/jvms/)

Experimental infection demonstrated that PaBV-2 first invades the central nervous system and then spreads to the systemic organs, and the distribution of inflammatory lesions and the virus in PaBV-infected birds changes during the time course of the infection [9, 10].

However, only a few studies have focused on the degree of inflammatory lesions in systemic organs in naturally PaBV-infected parrots [13–15, 20]. These reports noted the site of lesions but did not discuss variations in lesion distribution. We hypothesized that the degree of inflammation and lesion distribution would change with the infection stage in naturally PaBV-infected parrots. The purpose of this study was to clarify the link between the degree of inflammatory lesions in systemic organs and the distribution of the virus antigen in naturally PaBV-infected parrots. A study on the cardiac lesions of PaBV infection suggested a link between cardiac lesions and sudden death in PaBV-2-infected psittacine birds [11]. Thus, gross and microscopic findings of the heart were also investigated to determine if heart failure is an important symptom of PDD.

MATERIALS AND METHODS

Animals

From 2018 to 2020, necropsies were performed at Azabu University on 76 birds from two companion parrot breeding farms where endemic PaBV-2, 4, 7 infection was confirmed. PaBV was detected in 50 of 76 birds by reverse transcriptase-polymerase chain reaction (RT-PCR) in brain samples collected at necropsy using a previously reported method [7]. Histopathological examination was performed on 18 of the 50 birds that revealed mild postmortem changes (Table 1). Of the 18, 8 cases showed fewer postmortem changes (Case No. 1, 2, 6, 7, 8, 13, 14, 15) were subjected to detailed systemic pathological analysis. Skin was collected from the cervical region, and if the bird had feather loss, skin was collected from the area of feather loss. Proventriculus dilation was diagnosed if the stomach (proventriculus and ventriculus) occupied more than one-fourth of the body cavity. In evaluating congestion, the position of the body at the time of death was inferred by comparing the left and right color tones in the lungs and kidneys. Postmortem changes and effects of nonexsanguination were excluded. To grossly evaluate the heart, the maximum longitudinal and transverse diameters of the heart were measured and the longitudinal/transverse diameter ratio was calculated. The ratios in the 12 psittacine hearts that were PaBV negative on RT-PCR necropsied in our laboratory ranged from 1.4 to 1.8, with an average of 1.6. These hearts came from nine different kinds of psittacine birds, and all birds were adults. Values <1.3 were considered heart dilation, and values >1.4 were considered normal.

Histopathology and scoring

Samples collected during necropsy were fixed in 10% neutral-buffered formalin, embedded in paraffin, cut, and stained with hematoxylin and eosin. The brain and ventriculus were scored in all 18 cases, and other organs (spinal cord, peripheral nerve, crop, intestine, heart, lung, liver, kidney, and skin) were scored in 8 cases. In 10 cases, other organs were examined for the extent of mononuclear cell infiltration (Supplementary Table 1).

A previously published scoring method was modified for this study [9]. At least 10 high-power fields (2.37 mm^2) were evaluated in each brain section. The degree of inflammation (degree of perivascular cuffing and glial cell proliferation), lesion spread, and type of lesion (perivascular cuffing, glial cell proliferation, satellitosis, and neuronophagia) were each evaluated on a 3-point scale. The degree of perivascular cuffing inflammation was scored based on the number of cell layers surrounding the vessel, as follows: 1 point

Table 1. Case data and macroscopic findings

Case No.	Breed	Sex	Age	Isolated PaBV	Macroscopic findings					
					Crop dilation	Proventriculus dilation	Heart dilation	Pulmonary edema	Congestion	Feather loss
1	*Cacatua goffiniana*	F	Adult	PaBV7	+	+	-	-	Lung, Liver, Kidney	+
2	*Macaw* (*Mixed-breed*)	M	5y7m	PaBV4	+	+	+	+	Liver, Kidney	+
3	*Psittacus erithacus*	M	Adult	PaBV4	+	+	+	-	Lung, Liver, Kidney	-
4	*Aratinga solstitialis*	F	Adult	PaBV2,4	+	+	+	+	Lung, Liver, Kidney	+
5	*Psittacus erithacus*	F	Adult	PaBV4	+	+	-	-	Lung, Liver, Brain	-
6	*Aratinga weddellii*	M	Adult	PaBV4	+	+	+	-	Lung, Liver	+
7	*Amazona albifrons*	M	1y	PaBV4	+	+	+	-	Lung, Liver, Kidney	+
8	*Ara severus*	M	Adult	PaBV4	+	+	+	-	Spleen, Lung, Liver, Brain	+
9	*Bolborhynchus lineola*	M	2y	PaBV4	+	+	-	-	Spleen, Lung, Liver, kidney	-
10	*Ara chloropterus*	M	Adult	PaBV4	+	+	+	-	Spleen, Lung, Liver, kidney	+
11	*Cacatua galerita triton*	M	Adult	PaBV2,4	+	+	+	-	Lung, Liver, Kidney, Brain	-
12	*Ara ararauna*	M	7m	PaBV4	+	+	+	+	Spleen, Lung, Liver, kidney	-
13	*Anodorhynchus hyacinthinus*	M	Adult	PaBV4	+	+	+	-	Lung, Liver, Kidney	+
14	*Anodorhynchus hyacinthinus*	M	Adult	PaBV4	+	+	+	-	Lung, Liver, Kidney	+
15	*Deroptyus accipitrinus*	M	Adult	PaBV4	+	+	-	+	Spleen, Liver, Kidney	+
16	*Cacatua alba*	M	Adult	PaBV4	+	+	+	+	Lung, Liver, Kidney	+
17	*Ara ambiguus*	F	Adult	PaBV4	+	+	+	+	Lung, Liver, Kidney, Brain	-
18	*Poicephalus rueppellii*	F	3y	PaBV4	+	+	+	-	Lung, Liver, Kidney	-

F, female; M, male; PaBV, parrot bornavirus.

(1 layer), 2 points (2 layers), and 3 points (3 layers or more). Scores from at least 10 small vessels were averaged. The degree of glial cell proliferation was scored based on the proliferation pattern: 1 point (single cell infiltration), 2 points (accumulation of <4 cells), and 3 points (an accumulation of >4 cells). Lesion spread was scored as follows: 1 point (lesion only in the cerebrum or cerebellum; no >3 lesions), 2 points (local lesions in both the cerebrum and cerebellum; no >3 lesions in both the cerebrum and cerebellum), and 3 points (diffuse lesions in both the cerebrum and cerebellum; >4 lesions in both the cerebrum and cerebellum). The variety of lesions was scored as follows: 1 point (1 type of lesion observed), 2 points (2 types of lesions), and 3 points (3 or more types of lesions). The sum of all points was calculated (0–12 points).

Other organs (heart, lung, crop, stomach, intestine, liver, kidney, spinal cord, peripheral plexus, and skin) were evaluated for the degree of mononuclear cell infiltration and spread of the lesions. Histological sections with at least one plexus/nerve were used for evaluation, and at least 10 high-power fields (2.37 mm^2) were observed in each section. The degree of mononuclear cell infiltration was scored as follows: 1 point for mild inflammation (unicellular inflammatory cell infiltration), 2 points for moderate inflammation (<4 cell agglomerates were formed), and 3 points for severe inflammation (≥4 cell agglomerates were formed). Lesion spread was scored as follows: 1 point when inflammation was only part of the plexus, 2 points when inflammation was diffusely spread in the plexus, and 3 points when inflammation extended into the surrounding tissues, such as muscle and interstitium. The sum of all points was calculated (0–6 points).

To evaluate the heart, transverse sections of the heart were obtained and the epicardial ganglia/nerve, endocardium, myocardium, and Purkinje fibers were observed.

Immunohistochemistry and scoring

Paraffin sections were prepared using crest-coated glass slides (Matsunami Glass Ind., Ltd., Osaka, Japan). After deparaffinisation, the tissue sections were boiled in an Immunosaver (Nisshin EM Co., Tokyo, Japan), and endogenous peroxidase was blocked with 0.3% H_2O_2 in methanol to unmask the epitope. After blocking non-specific reactions with Block Ace (DS Pharma Biomedical, Osaka, Japan), tissue sections were incubated in primary antibody (anti-PaBV-5 phosphoprotein (P) rabbit serum) overnight at 4°C. Reactivity of the primary antibody to PaBV was confirmed by immunoblotting. After washing with phosphate-buffered saline (PBS), the sections were incubated with secondary antibodies (Hisfine Simple Stain MAX-PO, Multi, Nicherei Biosciences Inc., Tokyo, Japan), stained with diaminobenzidine (TaKaRa, Kusatsu, Japan), and counterstained with hematoxylin. Negative controls were incubated with rabbit serum instead of primary antibody.

The degree of positivity and spread of positive cells were evaluated for each organ. At least 10 high-power fields (2.37 mm^2) and more than one plexus/nerve were observed in each section. Compared with the negative control, the staining was considered negative only when the cytoplasm was weakly stained. When a clear granular positive image of the cytoplasm was obtained, it was considered positive. The degree of positive reaction was scored as follows: 1 point (weakly positive, the nucleus is weakly positive), 2 points (moderately positive, the nucleus is moderately to strongly positive and part of the cytoplasm is positive), and 3 points (strongly positive, the nucleus is strongly positive and the entire cytoplasm is positive). The spread of positive cells was scored as follows: 1 point (focal in some plexuses), 2 points (spread diffusely in the plexus), and 3 points (extending into the surrounding tissue, such as muscle or interstitium). The sum of all points was calculated (0–6 points).

Generation of in situ hybridisation (ISH) probes and ISH

ISH probes for PaBV were designed for the PaBV-4 nucleoprotein (N) genome (NCBI database accession No. NC_030688). Total RNA was extracted from frozen brains using an RNeasy Mini Kit (Qiagen, Hilden, Germany). The extracted RNA was used for cDNA synthesis using a SuperScript IV First-Strand Synthesis System (Thermo Fisher Scientific, Waltham, MA, USA). The cDNA was used for PCR (KOD FX: Toyobo, Tokyo, Japan) with the following PaBV primers: T7-tagged forward primer, 5′CCAAGCTTCTAATACGACTCACTATAGGGCCCCHCATGAGGCTATWGATTGGATTAACG3′; reverse primer, 5′GCMCGGTAGCCNGCCATTGTDGG 3′ [6]. The PCR product was isolated using a High Pure PCR Clean up Micro Kit (Nippon Genetics, Tokyo, Japan). The PCR product was cloned using a plasmid vector (pEX-K4J2), competent cells (DH5α: Toyobo, Tokyo, Japan), and Miniprep System (Promega, Tokyo, Japan). A DIG-labelled RNA probe (DIG RNA Labelling Mix, 10× conc: Sigma-Aldrich, St. Louis, MO, USA) was prepared using this T7-tagged PCR product.

Paraffin sections were prepared using crest-coated glass slides. ISH was performed with an IsHyb *In Situ* Hybridisation Kit (BioChain, San Francisco, CA, USA), following the manufacturer's instructions. Briefly, after deparaffinisation, the sections were fixed with 4% paraformaldehyde, washed with PBS, and treated with 0.1 mg/mL proteinase K at 37°C for 15 min. After washing with PBS, 4% paraformaldehyde was placed on the slides. The slides were then rinsed with distilled water, placed in the pre-hybridisation solution, and incubated at 50°C for 1 hr. The slides were then incubated in hybridisation solution containing the probe at 45°C overnight. Hybridisation without the probe was used as a negative control. The slides were subsequently washed with 2× saline sodium citrate, 1.5× saline sodium citrate, and 0.2× saline sodium citrate, and placed in blocking solution. Following treatment with alkaline phosphatase-labelled anti-DIG polyclonal goat antibody (Vector Laboratories, Inc., Newark, CA, USA), the slides were washed with PBS. Visualisation was performed using a Vector Red AP Substrate (Vector Laboratories, Inc.) and slides were counterstained with hematoxylin.

RESULTS

Macroscopic findings

A summary of the necropsy findings is shown in Table 1. Dilations of the crop, proventriculus, and/or ventriculus were observed in all 18 birds (Fig. 1), and dilation of the right ventricle was observed in 14 of 18 (78%) birds (Fig. 2). Congestion of multiple organs was observed in all 18 birds, and pulmonary edema was observed in 6 of 18 (33%) birds. No marked changes in the peripheral nerves (brachial plexus, synsacral plexus, or sciatic nerve) were observed. Feather loss was observed in 11 of 18 (61%) birds. No other infections were detected.

Histopathology

Glial cell proliferation accompanying rod cells, perivascular cuffing around small blood vessels, satellitosis, neuronophagia, and glial nodules were observed in the brains of all 18 birds (Fig. 3(a)–(c)). Mononuclear cell infiltration in the plexus distributed on the serosal surface and the intermuscular plexus was observed in the ventriculus in all 18 birds (Fig. 4(a)). Similarly, mononuclear infiltrates were also observed in the proventriculus, crop, and intestine.

The hearts were examined in 8 birds (Case No. 1, 2, 6, 7, 8, 13, 14, 15). Mononuclear cell infiltration was observed in the epicardial plexus of all 8 birds (Fig. 5(a)). Inflammatory cell infiltration between cardiac myocytes and surrounding blood vessels and myocardial degeneration was observed in 7 of 8 birds (Fig. 5(c)). Myocardial degeneration or necrosis was observed in 7 of 8 birds (Fig. 5(d)). Degeneration of the Purkinje fibers and mild endocardium fibrosis were observed in 1 bird each.

Inflammatory cells infiltrated the vessels of the liver and kidney in several cases (2/8 birds), and mononuclear cell infiltration around the bronchus in the lung was also observed in some cases (5/8 birds). In the spinal cord, inflammatory cells infiltrated the ganglia in all 8 birds. In the skin, mononuclear cell infiltration was observed around the plexus (6/8 birds), but inclusion bodies could not be confirmed in any tissue.

Histopathologic lesion distribution

Based on the distribution and degree of mononuclear cell infiltration, the 18 cases were classified into three types, as shown in Table 2 and Supplementary Table 2. In cases 1–5, the brain score was high and the stomach score was low. In cases 6–8, 11 and 12, both brain and stomach scores were high, and in cases 13–18, the brain score was low, but the stomach score was high. In case 9, both brain and stomach scores were low.

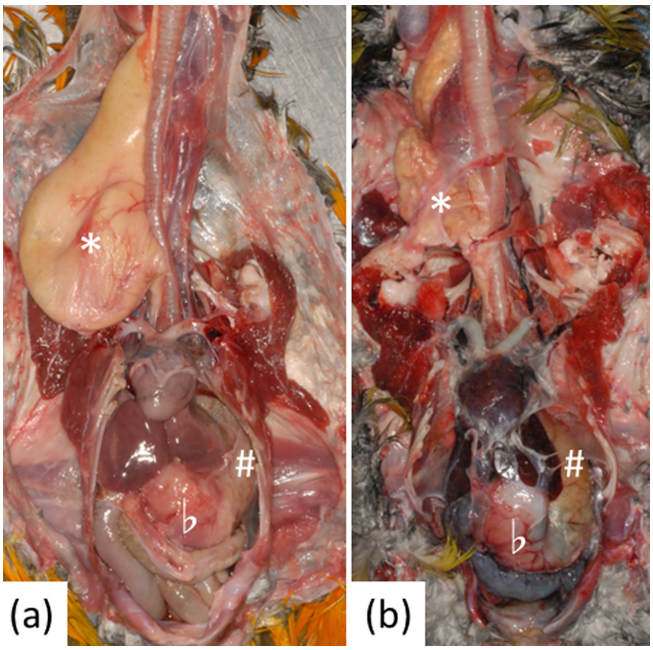

Fig. 1. Dilation of the crop, proventriculus, and ventriculus. * indicates the crop, # indicates the proventriculus, and b indicates the ventriculus. (**a**) Case 2. (**b**) Case 17.

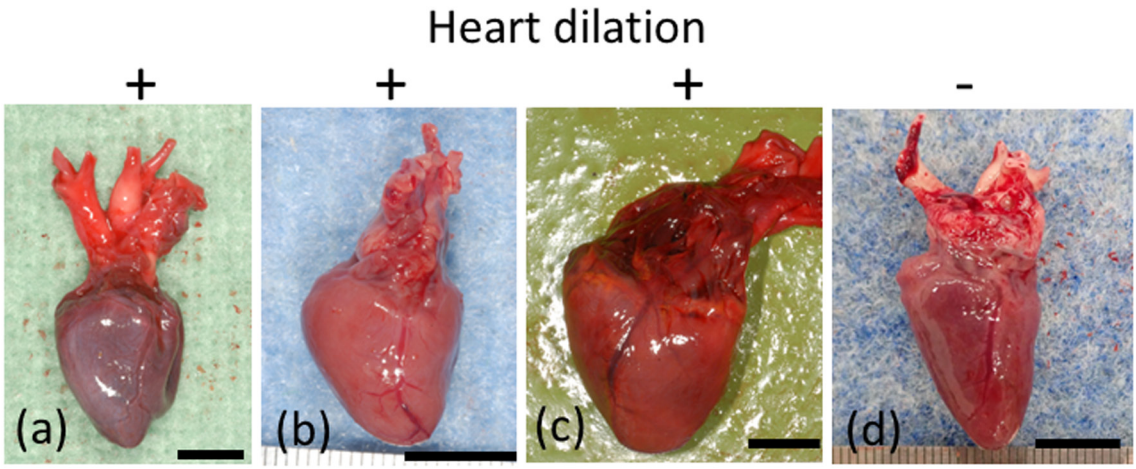

Fig. 2. Gross findings in the heart. Dilation of the right ventricle was observed (a–c). (**a**) Case 17. (**b**) Case 8. (**c**) Case 14. (**d**) Case 5. Bar=1 cm.

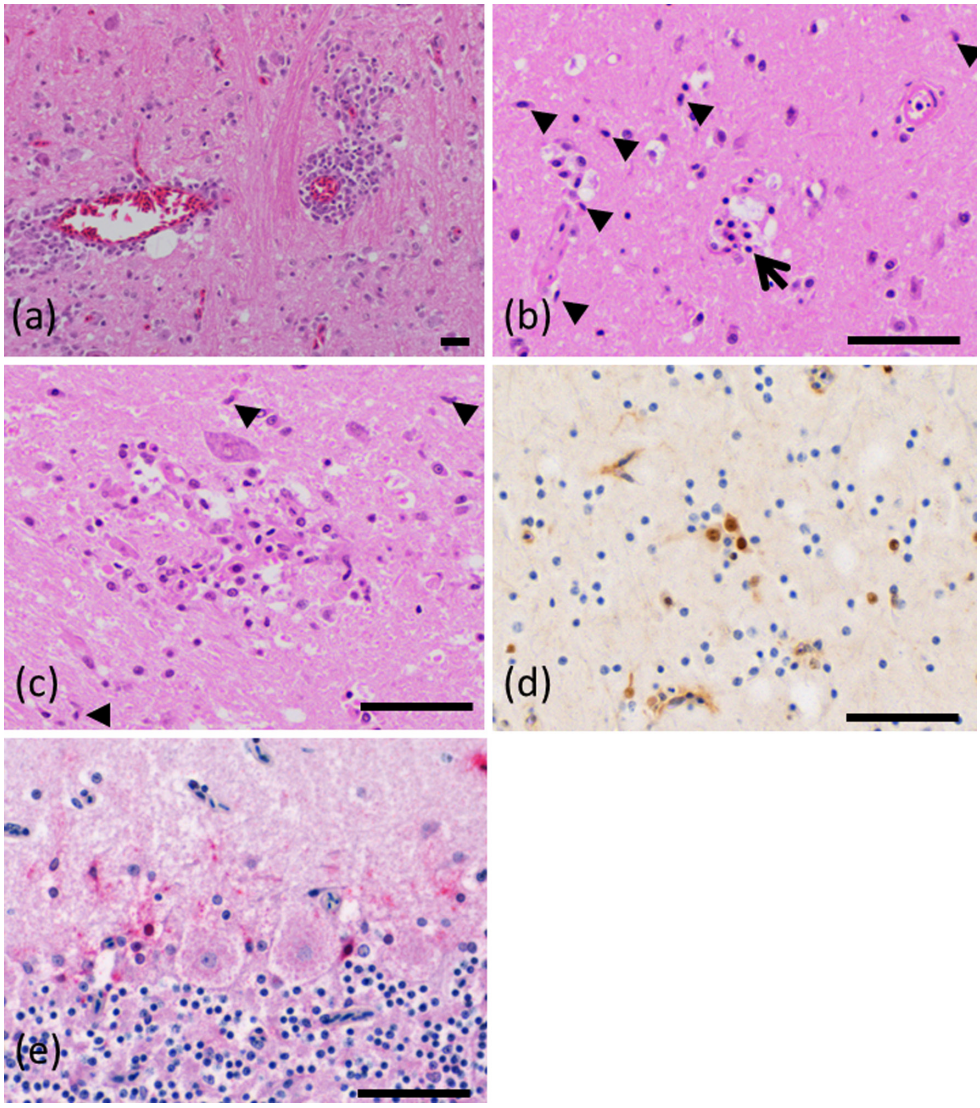

Fig. 3. Microscopic findings in the brain. (**a**) Perivascular cuffing and glial cell proliferation in the cerebrum in case 3 (hematoxylin and eosin). (**b**) Rod cells (arrowheads) and neuronophagia (arrow) in the cerebrum of case 2 (hematoxylin and eosin). (**c**) Glial nodule and rod cells (arrowheads) in the cerebrum of case 2 (hematoxylin and eosin). (**d**) Immunohistochemistry for parrot bornavirus (PaBV). A positive reaction was observed in the nuclei and cytoplasm in case 1. (**e**) Positive *in situ* hybridisation (ISH) reaction in the cerebellar piriform neurons in case 7. Bar=50 µm.

Immunohistochemistry

A positive reaction to PaBV antigen was observed in the brains of all 18 birds (Fig. 3(d)) and in the proventriculus and ventriculus of 17 of 18 (94%) birds (Fig. 4(b)). Systemic analysis was performed in 8 cases, and the results are shown in Table 3 and Supplementary Table 3. In the cerebellum, the nuclei and cytoplasm of piriform neurons exhibited particularly strong PaBV-positive staining. Purkinje cells were PaBV-negative. Ganglia in the spinal cord were strongly positive for PaBV. In the ventriculus, the intermuscular plexus and the serosal plexus were positive (Fig. 5(b)). In the heart, nerve cells and the nuclei and cytoplasm of cardiac myocytes were positive (Fig. 5(e)). Lung neurons were also PaBV-positive in most cases (6/8). The liver and kidneys were PaBV-negative in all 8 cases. Positive cells were detected in inflammatory lesions of the skin to varying degrees in all 8 cases.

As shown in Table 3, the brain score was high, but the stomach score was low in cases 1 and 2. In cases 6–8, both brain and stomach scores were high. In cases 13–15, the brain score was low, but the stomach score was high.

ISH

A summary of the ISH results is shown in Table 4. The nucleus and cytoplasm of the neurons in the cerebral parenchyma were positive for PaBV RNA. The nucleus and cytoplasm of the piriform neurons in the cerebellum were also positive for PaBV (Fig. 3(e)). The virus was detected in both the cell bodies and dendrites of neurons. Consistent with the immunolabeling, ISH for PaBV RNA was negative in Purkinje cells. The nuclei and cytoplasm of nerve cells in the intermuscular plexus and serosal plexus of the ventriculus

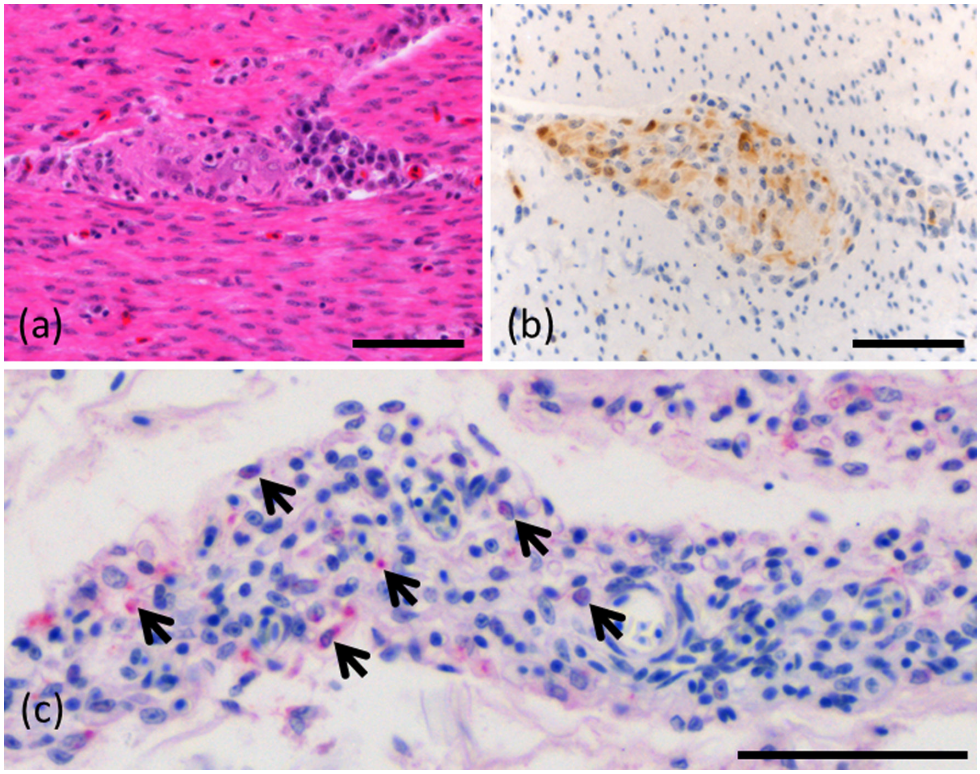

Fig. 4. Microscopic findings in the ventriculus. (**a**) Inflammatory cell infiltration of the intermuscular plexus of the pars muscularis in case 6 (hematoxylin and eosin). (**b**) Immunohistochemistry for parrot bornavirus (PaBV). A positive reaction was observed in the nuclei and cytoplasm in case 6. (**c**) Positive *in situ* hybridisation (ISH) reaction (arrows) in the nucleus and cytoplasm in the serosal plexus of case 7. Bar=50 µm.

were positive (Fig. 4(c)). The nuclei and cytoplasm of the epicardial plexus of the heart and some cardiomyocytes were also positive (Fig. 5(f)). No positive cells were observed in the liver and kidneys examined. Nerve cells in the skin plexus were positive.

As shown in Table 4, cases 1 and 2 were positive in the brain, spinal cord, stomach, and heart, but negative in peripheral nerves, crop, intestine, lung, liver, and kidney. Cases 6–8 and 13–15 were positive in almost all systemic organs other than the liver and kidney.

DISCUSSION

The pathological findings in this study were consistent with previous reports concerning natural PaBV infections in parrots [14, 15, 18, 19]. Based on the results of the present study, parrots naturally infected with PaBV can be classified into three types of lesions distribution based on brain and digestive histopathologic findings. In the neural type, immunohistochemical and ISH findings, a strong and diffusely positive reaction in the brain, and a negative or weakly positive reaction in the stomach were consistent with the histopathological findings. In the digestive type, immunolabeling for PaBV was strongly positive in the stomach and weakly positive in the brain. The neural/digestive type had significant inflammation in both the stomach and brain, and immunolabeling was strongly positive in both tissues. These findings indicate that the distribution of lesions corresponded closely with the PaBV distribution. This variation in the distribution of lesions and the virus in naturally-infected parrots is a novel finding that may help determine the pathogenesis of PaBV infection.

Experimental infections with PaBV-2 showed that the distribution of viral antigen and inflammatory lesions changes over the time course of PaBV infection. The infection first invades the brain, and then spreads to the peripheral nerves [9, 10]. In addition, brain inflammation becomes milder over time after experimental infection, and recovery is likely to occur as the viral load decreases in the late stages of infection [9, 10]. The classification of lesions in naturally PaBV-infected cases may be explained by the progression of the infection over time. PaBVs, which primarily affect nerves, enter the central nervous system (neural type), then spreads to peripheral nerves (neural/digestive type), progressing to the digestive type. Case 9 showed weak degree of macroscopic findings, histopathological and immunohistochemical scores in the brain and stomach. This case 9 was classified as unclassified because it was not classified into each of the three types. It could not be determined whether the extent of lesions in this case was weak or whether the changes were due to the time course of PaBV infection. Since this study was an analysis of naturally-infected cases, the time of infection was uncertain, detailed information on the course of symptoms was not available, and the route of infection may be different between experimental and natural infections. The role of age reported at the time of infection has previously been reported [2]. Age may have also influenced lesion distribution in our study. Further research is necessary to better delineate the progression of the disease.

Previous studies also reported mononuclear cell infiltration in the heart and viral localisation in the plexus and/or myocardial fibers

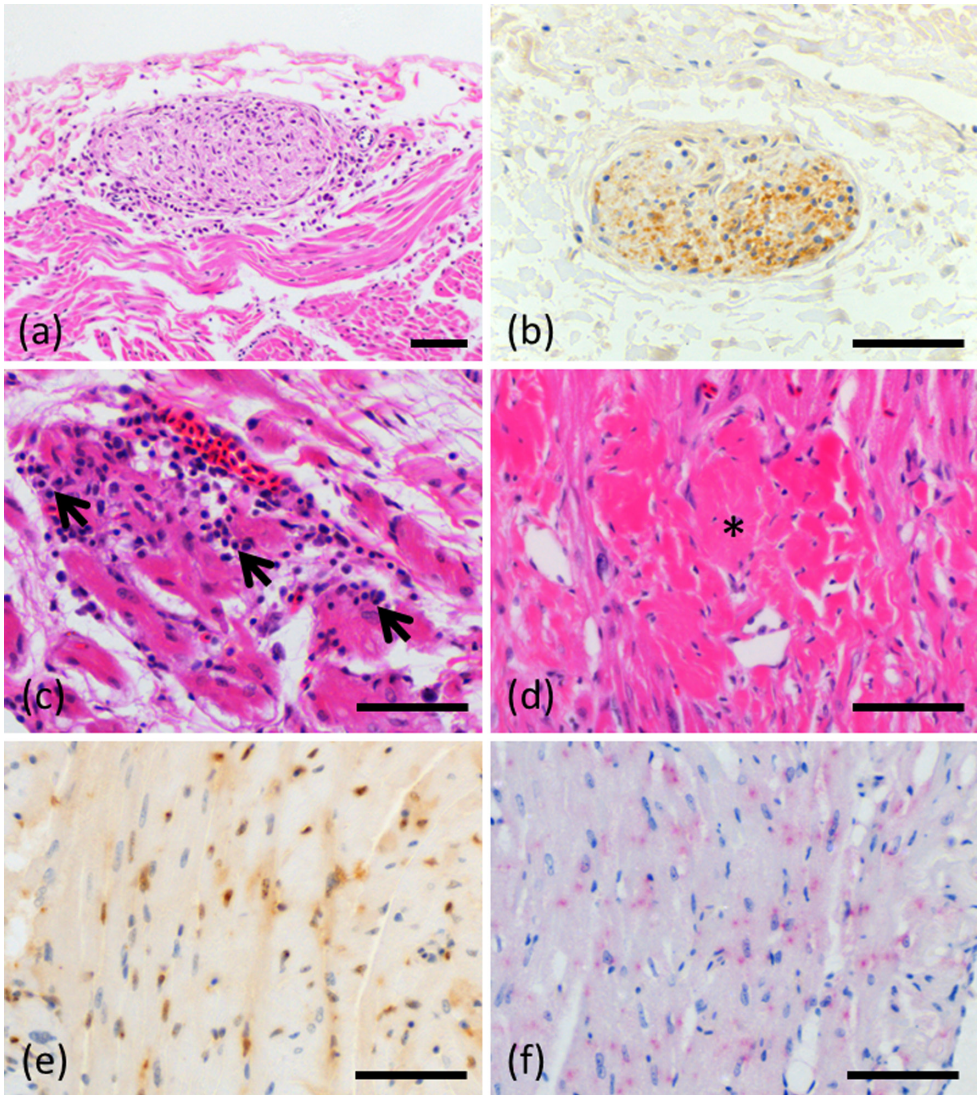

Fig. 5. Microscopic findings in the heart. (**a**) Inflammatory cell infiltration of the epicardial plexus in case 2 (hematoxylin and eosin). (**b**) Immunohistochemistry for parrot bornavirus (PaBV). Positive cells in the epicardial plexus in case 2. (**c**) Mononuclear cell infiltration (arrows) between cardiac myocytes in case 8 (hematoxylin and eosin). (**d**) Myocardial degeneration (asterisk) in case 8 (hematoxylin and eosin). (**e**) Immunohistochemistry for PaBV. A positive reaction was observed in the nuclei and cytoplasm of cardiac myocytes in case 8. (**f**) Positive *in situ* hybridisation (ISH) reaction was observed in the nuclei and cytoplasm of cardiac myocytes in case 8. Bar=50 µm.

in PaBV-2 or -4-infected parrots [18, 19]. These reports only noted the presence of the virus and did not discuss its significance in the pathogenesis of the disease. A link was indicated between cardiac disease lesions and sudden death in PaBV-2-infected psittacine birds recently [11]. In the present study, dilation of the right ventricle was observed in 78% (14/18) of cases, congestion of multiple organs was observed in all cases (18/18), and histopathological examination revealed the virus in cardiac myocytes in all cases (8/8). Unlike other organs, ganglioneuritis, cardiac myocyte infection, myocardial degeneration, and myocarditis were observed in the heart. This suggests that cardiac trophism of PaBV and heart failure were the causes of death in birds infected with PaBV. The symptoms of PDD from PaBV infection include malnutrition due to gastrointestinal symptoms, neurological symptoms, and sudden death without obvious symptoms [6]. Our results indicate that heart failure should also be considered an important symptom of PDD. Heart lesions were observed in parrots infected with any of the three types of PaBV infection (PaBV-4, -2/-4, and -7), and sudden death by heart failure could occur at any time in the course of PaBV infection.

In the present study, PaBV-7 was detected in a *Cacatua goffiniana* (case 1). Although PaBV-7 was isolated from this species [17], the detailed pathological findings of PaBV-7 infection were not described. The PaBV-7-infected bird in this report had mild lesions in the stomach and severe lesions in the brain. Whether the location of lesions was related to the virus type or the time of infection is unclear. Further research with multiple cases is necessary to clarify these issues.

PaBV infection is primarily diagnosed by genetic testing of faecal or rectal swabs [3, 12]. However, some birds in the present study had almost no lesions and little virus in the digestive system. Therefore, PCR of faecal/rectal may be negative depending on the

Table 2. Scoring of microscopic findings

Case No.	Type	Brain	Spinal cord	Peripheral nerve	Crop	Ventriculus	Intestine	Heart	Lungs	Liver	Kidney	Skin
1	Neural	12	3	3	2	4	2	2	0	0	0	0
2	Neural	12	4	3	2	3	2	3	2	0	0	0
3	Neural	9	ND	ND	ND	2	ND	ND	ND	ND	ND	ND
4	Neural	8	ND	ND	ND	2	ND	ND	ND	ND	ND	ND
5	Neural	12	ND	ND	ND	4	ND	ND	ND	ND	ND	ND
6	Neural/digestive	11	5	3	6	6	4	3	2	2	0	2
7	Neural/digestive	12	3	2	4	5	4	4	0	0	2	3
8	Neural/digestive	12	5	4	4	6	6	5	3	0	3	3
9	Unclassified	6	ND	ND	ND	3	ND	ND	ND	ND	ND	ND
10	Neural/digestive	10	ND	ND	ND	6	ND	ND	ND	ND	ND	ND
11	Neural/digestive	10	ND	ND	ND	5	ND	ND	ND	ND	ND	ND
12	Neural/digestive	10	ND	ND	ND	6	ND	ND	ND	ND	ND	ND
13	Digestive	7	6	3	3	6	6	5	0	0	0	4
14	Digestive	5	5	2	3	5	5	4	2	0	0	3
15	Digestive	6	5	3	6	6	6	4	2	2	0	4
16	Digestive	5	ND	ND	ND	4	ND	ND	ND	ND	ND	ND
17	Digestive	8	ND	ND	ND	6	ND	ND	ND	ND	ND	ND
18	Digestive	7	ND	ND	ND	5	ND	ND	ND	ND	ND	ND

ND, not determined.

Table 3. Immunohistochemical scoring of parrot bornavirus (PaBV) antigens

Case No.	Type	Brain	Spinal cord	Peripheral nerve	Crop	Ventriculus	Intestine	Heart	Lungs	Liver	Kidney	Skin
1	Neural	6	6	4	0	0	0	4	0	0	0	2
2	Neural	6	5	5	2	2	2	4	0	0	0	2
6	Neural/digestive	6	5	6	5	6	6	6	5	0	0	4
7	Neural/digestive	5	5	5	5	5	5	5	3	0	0	5
8	Neural/digestive	6	6	4	5	5	5	6	4	0	0	3
13	Digestive	3	5	4	4	6	6	6	4	0	0	4
14	Digestive	3	6	5	5	6	6	5	5	0	0	3
15	Digestive	4	6	5	5	6	6	6	3	0	0	4

Table 4. Result of *in situ* hybridization

Case No.	Type	Brain	Spinal cord	Peripheral nerve	Crop	Ventriculus	Intestine	Heart	Lungs	Liver	Kidney	Skin
1	Neural	+	+	-	-	+	-	+	-	-	-	+
2	Neural	+	+	-	-	+	-	+	-	-	-	+
6	Neural/digestive	+	+	+	+	+	+	+	+	-	-	-
7	Neural/digestive	+	+	+	+	+	+	+	+	-	-	+
8	Neural/digestive	+	+	+	+	+	+	+	+	-	-	-
13	Digestive	+	+	+	+	+	+	+	+	-	-	-
14	Digestive	+	+	+	+	+	+	+	+	-	-	+
15	Digestive	+	+	+	-	+	-	-	+	-	-	+

+: positive; -: negative.

sampling site or the stage of infection. Our results indicate that the viral distribution varies in across cases of natural PaBV infection, so multiple examinations at different times or different sites (for example, skin and faeces) are necessary to accurately detect PaBV infection.

CONFLICT OF INTEREST. The authors report there are no competing interests to declare.

REFERENCES

1. Berhane Y, Smith DA, Newman S, Taylor M, Nagy E, Binnington B, Hunter B. 2001. Peripheral neuritis in psittacine birds with proventricular dilatation disease. *Avian Pathol* **30**: 563–570. [Medline] [CrossRef]
2. Gartner AM, Link J, Bücking B, Enderlein D, Herzog S, Petzold J, Malberg S, Herden C, Lierz M. 2021. Age-dependent development and clinical characteristics of an experimental parrot bornavirus-4 (PaBV-4) infection in cockatiels (*Nymphicus hollandicus*). *Avian Pathol* **50**: 138–150. [Medline] [CrossRef]
3. Heffels-Redmann U, Enderlein D, Herzog S, Piepenbring A, Bürkle M, Neumann D, Herden C, Lierz M. 2012. Follow-up investigations on different courses of natural avian bornavirus infections in psittacines. *Avian Dis* **56**: 153–159. [Medline] [CrossRef]
4. Honkavuori KS, Shivaprasad HL, Williams BL, Quan PL, Hornig M, Street C, Palacios G, Hutchison SK, Franca M, Egholm M, Briese T, Lipkin WI. 2008. Novel borna virus in psittacine birds with proventricular dilatation disease. *Emerg Infect Dis* **14**: 1883–1886. [Medline] [CrossRef]
5. Hoppes SM, Tizard I, Shivaprasad HL. 2013. Avian bornavirus and proventricular dilatation disease: diagnostics, pathology, prevalence, and control. *Vet Clin North Am Exot Anim Pract* **16**: 339–355. [Medline] [CrossRef]
6. Kistler AL, Gancz A, Clubb S, Skewes-Cox P, Fischer K, Sorber K, Chiu CY, Lublin A, Mechani S, Farnoushi Y, Greninger A, Wen CC, Karlene SB, Ganem D, DeRisi JL. 2008. Recovery of divergent avian bornaviruses from cases of proventricular dilatation disease: identification of a candidate etiologic agent. *Virol J* **5**: 88. [Medline] [CrossRef]
7. Komorizono R, Tomonaga K, Makino A. 2020. Development of a reverse transcription-loop-mediated isothermal amplification assay for the detection of parrot bornavirus 4. *J Virol Methods* **275**: 113749. [Medline] [CrossRef]
8. Kuhn JH, Adkins S, Agwanda BR, Al Kubrusli R, Alkhovsky SV, Amarasinghe GK, Avšič-Županc T, Ayllón MA, Bahl J, Balkema-Buschmann A, Ballinger MJ, Basler CF, Bavari S, Beer M, Bejerman N, Bennett AJ, Bente DA, Bergeron É, Bird BH, Blair CD, Blasdell KR, Blystad DR, Bojko J, Borth WB, Bradfute S, Breyta R, Briese T, Brown PA, Brown JK, Buchholz UJ, Buchmeier MJ, Bukreyev A, Burt F, Büttner C, Calisher CH, Cao M, Casas I, Chandran K, Charrel RN, Cheng Q, Chiaki Y, Chiapello M, Choi IR, Ciuffo M, Clegg JCS, Crozier I, Dal Bó E, de la Torre JC, de Lamballerie X, de Swart RL, Debat H, Dheilly NM, Di Cicco E, Di Paola N, Di Serio F, Dietzgen RG, Digiaro M, Dolnik O, Drebot MA, Drexler JF, Dundon WG, Duprex WP, Dürrwald R, Dye JM, Easton AJ, Ebihara H, Elbeaino T, Ergünay K, Ferguson HW, Fooks AR, Forgia M, Formenty PBH, Fránová J, Freitas-Astúa J, Fu J, Fürl S, Gago-Zachert S, Gão GF, García ML, García-Sastre A, Garrison AR, Gaskin T, Gonzalez JJ, Griffiths A, Goldberg TL, Groschup MH, Günther S, Hall RA, Hammond J, Han T, Hepojoki J, Hewson R, Hong J, Hong N, Hongo S, Horie M, Hu JS, Hu T, Hughes HR, Hüttner F, Hyndman TH, Ilyas M, Jalkanen R, Jiāng D, Jonson GB, Junglen S, Kadono F, Kaukinen KH, Kawate M, Klempa B, Klingström J, Kobinger G, Koloniuk I, Kondō H, Koonin EV, Krupovic M, Kubota K, Kurath G, Laenen L, Lambert AJ, Langevin SL, Lee B, Lefkowitz EJ, Leroy EM, Li S, Li L, Lǐ J, Liu H, Lukashevich IS, Maes P, de Souza WM, Marklewitz M, Marshall SH, Marzano SL, Massart S, McCauley JW, Melzer M, Mielke-Ehret N, Miller KM, Ming TJ, Mirazimi A, Mordecai GJ, Mühlbach HP, Mühlberger E, Naidu R, Natsuaki T, Navarro JA, Netesov SV, Neumann G, Nowotny N, Nunes MRT, Olmedo-Velarde A, Palacios G, Pallás V, Pályi B, Papa A, Paraskevopoulou S, Park AC, Parrish CR, Patterson DA, Pauvolid-Corrêa A, Pawęska JT, Payne S, Peracchio C, Pérez DR, Postler TS, Qi L, Radoshitzky SR, Resende RO, Reyes CA, Rima BK, Luna GR, Romanowski V, Rota P, Rubbenstroth D, Rubino L, Runstadler JA, Sabanadzovic S, Sall AA, Salvato MS, Sang R, Sasaya T, Schulze AD, Schwemmle M, Shi M, Shí X, Shí Z, Shimomoto Y, Shirako Y, Siddell SG, Simmonds P, Sironi M, Smagghe G, Smither S, Song JW, Spann K, Spengler JR, Stenglein MD, Stone DM, Sugano J, Suttle CA, Tabata A, Takada A, Takeuchi S, Tchouassi DP, Teffer A, Tesh RB, Thornburg NJ, Tomitaka Y, Tomonaga K, Tordo N, Torto B, Towner JS, Tsuda S, Tu C, Turina M, Tzanetakis IE, Uchida J, Usugi T, Vaira AM, Vallino M, van den Hoogen B, Varsani A, Vasilakis N, Verbeek M, von Bargen S, Wada J, Wahl V, Walker PJ, Wang LF, Wang G, Wang Y, Wang Y, Waqas M, Wèi T, Wen S, Whitfield AE, Williams JV, Wolf YI, Wu J, Xu L, Yanagisawa H, Yang C, Yang Z, Zerbini FM, Zhai L, Zhang YZ, Zhang S, Zhang J, Zhang Z, Zhou X. 2021. 2021 Taxonomic update of phylum Negarnaviricota (Riboviria: Orthornavirae), including the large orders Bunyavirales and Mononegavirales. *Arch Virol* **166**: 3513–3566. [Medline] [CrossRef]
9. Leal de Araujo J, Rodrigues-Hoffmann A, Giaretta PR, Guo J, Heatley J, Tizard I, Rech RR. 2019. Distribution of viral antigen and inflammatory lesions in the central nervous system of cockatiels (*Nymphicus hollandicus*) experimentally infected with parrot bornavirus 2. *Vet Pathol* **56**: 106–117. [Medline] [CrossRef]
10. Leal de Araujo J, Rech RR, Heatley JJ, Guo J, Giaretta PR, Tizard I, Rodrigues-Hoffmann A. 2017. From nerves to brain to gastrointestinal tract: A time-based study of parrot bornavirus 2 (PaBV-2) pathogenesis in cockatiels *(Nymphicus hollandicus*). *PLoS One* **12**: e0187797. [Medline] [CrossRef]
11. Leal de Araujo J, Hameed SS, Tizard I, Escandon P, Giaretta PR, Heatley JJ, Hoppes S, Rech RR. 2020. Cardiac lesions of natural and experimental infection by parrot bornaviruses. *J Comp Pathol* **174**: 104–112. [Medline] [CrossRef]
12. Leal de Araújo J, Rech RR. 2021. Seeing beyond a dilated proventriculus: Diagnostic tools for proventricular dilatation disease in psittacine birds. *Animals (Basel)* **11**: 3558. [Medline] [CrossRef]
13. Ogawa H, Sanada Y, Sanada N, Kudo M, Tuchiya K, Kodama T, Uetsuka K. 2011. Proventricular dilatation disease associated with avian bornavirus infection in a Citron-crested Cockatoo that was born and hand-reared in Japan. *J Vet Med Sci* **73**: 837–840. [Medline] [CrossRef]
14. Ouyang N, Storts R, Tian Y, Wigle W, Villanueva I, Mirhosseini N, Payne S, Gray P, Tizard I. 2009. Histopathology and the detection of avian bornavirus in the nervous system of birds diagnosed with proventricular dilatation disease. *Avian Pathol* **38**: 393–401. [Medline] [CrossRef]
15. Raghav R, Taylor M, Delay J, Ojkic D, Pearl DL, Kistler AL, Derisi JL, Ganem D, Smith DA. 2010. Avian bornavirus is present in many tissues of psittacine birds with histopathologic evidence of proventricular dilatation disease. *J Vet Diagn Invest* **22**: 495–508. [Medline] [CrossRef]
16. Rubbenstroth D. 2022. Avian bornavirus research-a comprehensive review. *Viruses* **14**: 1513. [Medline] [CrossRef]
17. Rubbenstroth D, Rinder M, Kaspers B, Staeheli P. 2012. Efficient isolation of avian bornaviruses (ABV) from naturally infected psittacine birds and identification of a new ABV genotype from a salmon-crested cockatoo (*Cacatua moluccensis*). *Vet Microbiol* **161**: 36–42. [Medline] [CrossRef]
18. Weissenböck H, Fragner K, Nedorost N, Mostegl MM, Sekulin K, Maderner A, Bakonyi T, Nowotny N. 2010. Localization of avian bornavirus RNA by in situ hybridization in tissues of psittacine birds with proventricular dilatation disease. *Vet Microbiol* **145**: 9–16. [Medline] [CrossRef]
19. Weissenböck H, Bakonyi T, Sekulin K, Ehrensperger F, Doneley RJT, Dürrwald R, Hoop R, Erdélyi K, Gál J, Kolodziejek J, Nowotny N. 2009. Avian bornaviruses in psittacine birds from Europe and Australia with proventricular dilatation disease. *Emerg Infect Dis* **15**: 1453–1459. [Medline] [CrossRef]
20. Wünschmann A, Honkavuori K, Briese T, Lipkin WI, Shivers J, Armien AG. 2011. Antigen tissue distribution of Avian bornavirus (ABV) in psittacine birds with natural spontaneous proventricular dilatation disease and ABV genotype 1 infection. *J Vet Diagn Invest* **23**: 716–726. [Medline] [CrossRef]